Manconi, A., Walter, T. R., Manzo, M., Zeni, G., Tizzani, P., Sansosti, E., Lanari, R. (2010): On the effects of 3-D mechanical heterogeneities at Campi Flegrei caldera, southern Italy. - Journal of Geophysical Research, 115, B08405

DOI: 10.1029/2009JB007099

On the effects of 3-D mechanical heterogeneities at Campi Flegrei caldera, southern Italy

Andrea Manconi,[1,2] Thomas R. Walter,[1] Mariarosaria Manzo,[2] Giovanni Zeni,[2] Pietro Tizzani,[2] Eugenio Sansosti,[2] and Riccardo Lanari[2]

Received 3 November 2009; revised 3 March 2010; accepted 2 April 2010; published 14 August 2010.

[1] Campi Flegrei caldera, located near the highly populated city of Naples, southern Italy, is characterized by long-term subsidence punctuated by fast uplift phases. Most of the interpretations of the ground deformation are still based on standard models that assume the lithosphere to behave as a homogeneous half-space. However, several geophysical investigations show the presence of vertical and lateral heterogeneities, especially in the shallow subsurface, which might have an effect on the interpretation of the surface displacements. Our 3-D finite element models, constrained by seismic tomography to take into account the realistic distribution of mechanical heterogeneities, demonstrate that at Campi Flegrei the assessment of the source location is independent of the consideration of 3-D heterogeneities, while the evaluation of its strength is overestimated. Thus, we propose an approach that still allows use of standard homogeneous half-space models but accounts for 3-D heterogeneity effects. This procedure, applied to the deformation field revealed by Differential Synthetic Aperture Radar Interferometry (DInSAR) over the past 16 years, provides new insights for the understanding of the ground displacements observed at Campi Flegrei caldera. This work provides an approach for a quantitative evaluation of the effects of mechanical heterogeneities on surface deformation. Analogous procedures can be also applied in other volcanic areas where, similar to Campi Flegrei caldera, a priori information on the mechanical heterogeneities distribution is available.

Citation: Manconi, A., T. R. Walter, M. Manzo, G. Zeni, P. Tizzani, E. Sansosti, and R. Lanari (2010), On the effects of 3-D mechanical heterogeneities at Campi Flegrei caldera, southern Italy, *J. Geophys. Res.*, *115*, B08405, doi:10.1029/2009JB007099.

1. Introduction

[2] Ground deformation in volcanic areas is the surface expression of deep-seated physical processes, which might be related to renewed magma emplacement or to changes within a pre-existing magmatic and/or hydrothermal reservoir. The study of the surface displacement helps to understand the source at depth, constraining parameters such as the location, the shape, and volume/pressure changes, which are indispensable for the assessment of a volcanic hazard potential [*Dzurisin*, 2006]. The analysis of the deformation signal is usually performed by setting up inverse problems, which consider simple source models embedded in a homogeneous half-space. However, recent studies have shown that the hypothesis of homogeneity in volcanic areas is often an oversimplification that might lead to misinterpretations of the retrieved source parameters [*Trasatti et al.*, 2005; *Crescentini and Amoruso*, 2007; *Manconi et al.*, 2007; *Masterlark*, 2007].

[3] Nevertheless, the consideration of homogeneous distribution of mechanical properties in volcano deformation studies is still the "standard" approach.

[4] Campi Flegrei (CF) is a caldera system located near the city of Naples, southern Italy, where in the last 30 years a number of geophysical investigations provided important constraints relevant to the subsurface structure. In particular, these analyses clearly identify the contrast between the external rim of the caldera, characterized by mechanically stiffer material, and the internal caldera basin structure, composed by softer and incoherent sediments [*De Natale et al.*, 2006, and references therein]. In this work, we include such distribution of the mechanical properties in 3-D heterogeneous finite element models of CF caldera. The principal aims of this paper are (1) to show the implications of the consideration of a simplified homogeneous model for the interpretation of the deformation field at CF caldera and (2) to propose a fast and reliable methodology to take into account the effects of mechanical heterogeneities.

[5] The paper is organized as follows. After a brief introduction on CF caldera and its recent unrest history, we describe the implementation of 3-D heterogeneous finite

[1]Department of Physics of the Earth, GFZ German Research Centre for Geoscience, Potsdam, Germany.
[2]Istituto per il Rilevamento Elettromagnetico dell'Ambiente, Consiglio Nazionale delle Ricerche, Naples, Italy.

0148-0227/10/2009JB007099

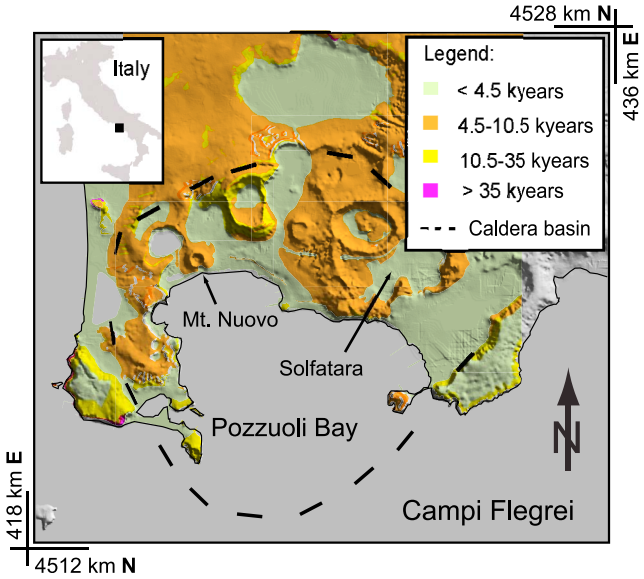

Figure 1. Sketch of the geological map superimposed on the digital elevation model of the Campi Flegrei caldera. The inner caldera basin (dashed black line) is composed mostly of Quaternary soft materials and young volcanic deposits.

element models, with the elastic mechanical properties constrained by means of available seismic tomography information. Then, we detail the synthetic tests performed to assess the capability of simplified homogeneous models to attain a reliable solution when a more complex heterogeneity distribution is considered. The results show that the consideration of a realistic distribution of mechanical heterogeneities at CF caldera has major effects only on the estimation of the source volume change. Hence, we propose a method to retrieve the source parameters "corrected" for the 3-D heterogeneity effects. Finally, we apply this method to the analysis of the past 16 year deformation at CF caldera exploited via the Small BAseline Subset (SBAS) approach, an advanced DInSAR technique that allows the exploitation of mean deformation velocity maps and displacement time series [*Berardino et al.*, 2002].

[6] CF caldera (Figure 1) is a ~12 km wide collapse structure formed by two major eruptions: the Campanian Ignimbrite and the Neapolitan Yellow Tuff (39 ka BP, VEI = 7 and 15 ka BP, VEI = 6, respectively [*Mastrolorenzo and Pappalardo*, 2006]). In the post-caldera phase, the activity in the area has been characterized by long-term subsidence punctuated by fast uplifts phases. The latest eruptive event occurred in 1538 AD (Monte Nuovo eruption), following a ground uplift of several meters [*Bellucci et al.*, 2006]. In recent times, the most important unrest occurred between 1969 and 1971 and 1982–1984, when the city of Pozzuoli raised in total of about 3.5 m [*De Natale et al.*, 1991]. The surface displacements have been accompanied by several earthquakes, which caused severe damages to the buildings and the subsequent evacuation of 40,000 people [*Bianco et al.*, 2004]. Since 1985, the subsidence trend has re-started, interrupted by uplifts of smaller amplitude in 1989, 1996, 2000–2001 and 2004–2006, with the last two accompanied again by considerable seismic swarms [*Chiodini*, 2009].

[7] The surface deformation at CF caldera is currently monitored by using ground-based (e.g., EDM, leveling) and space-based geodetic techniques (GPS, DInSAR). A number of authors analyzed the geodetic signals in order to characterize the source responsible for the subsidence and the uplift phases at CF caldera [e.g., *De Natale et al.*, 1991; *Lundgren et al.*, 2001; *Lanari et al.*, 2004; *De Natale et al.*, 2006, and references therein; *Gottsmann et al.*, 2006; *Bodnar et al.*, 2007; *Trasatti et al.*, 2008, and references therein; *Amoruso et al.*, 2008, and references therein]. While there is a general agreement on the source location, beneath the center of the caldera between 2.5 and 3.5 km depth, parameters as geometry, dimensions, strength and nature (magmatic, hydrothermal or hybrid) of the reservoir strongly depend in turn on the analyzed data set and on the considered modeling assumptions. Thus, a comprehensive explanation of the long-term as well as the short-term ground deformation pattern is currently a matter of discussion. More than 3 million people live in the surrounding of CF caldera, considering the city of Naples and sub-urban area, making this volcanic region one of the most hazardous on Earth [*De Natale et al.*, 2006]. Therefore, a fast, precise and reliable assessment of the source parameters is important not only for the general understanding of the geodetic signal related to volcanic processes, but also crucial for volcanic hazard assessment.

2. Finite Element Models of CF Caldera: Setup

[8] The finite element (FE) models used in this study are three dimensional, 200x200x100 km respectively in the east (E), north (N) and z (positive downward) directions (Figure 2a). The performance of the discretization, ~17,000 tetrahedral elements, has been verified through convergence tests [*Fagan*, 1992], finding that a higher resolution would affect the surface displacements of values smaller than accuracies achievable with standard geodetic techniques (<0.1 mm) (see the auxiliary material).[1] The topographic relief of CF caldera (altitude < 0.4 km) has only a minor influence on the displacement field; hence it is not considered in the FE models [*Cayol and Cornet*, 1998]. Mechanical properties for the 3-D heterogeneous FE models (hereafter referred to as 3DHET) have been extrapolated from the seismic tomography study presented by *Chiarabba and Moretti* [2006], whose results are in agreement with the other geophysical studies performed in the area and, moreover, provide an unprecedented detail of the shallow subsurface in the inner part of the caldera. The elastic constants are calculated by using the empirical relationship between seismic velocities and mechanical parameters proposed by *Brocher* [2005]. The resulting values of the shear moduli (μ) and Poisson's ratios (ν) in the first 4 km of the subsurface at CF caldera are in the range of 2–14 GPa and 0.2–0.4, respectively (Figure 2b).

2.1. Synthetic Tests

[9] In order to evaluate the effects of the 3-D distribution of mechanical properties, we applied the following steps. We simulated a positive volume change (ΔV) of 1 Mm^3

[1] Auxiliary materials are available in the HTML. doi:10.1029/2009JB007099.

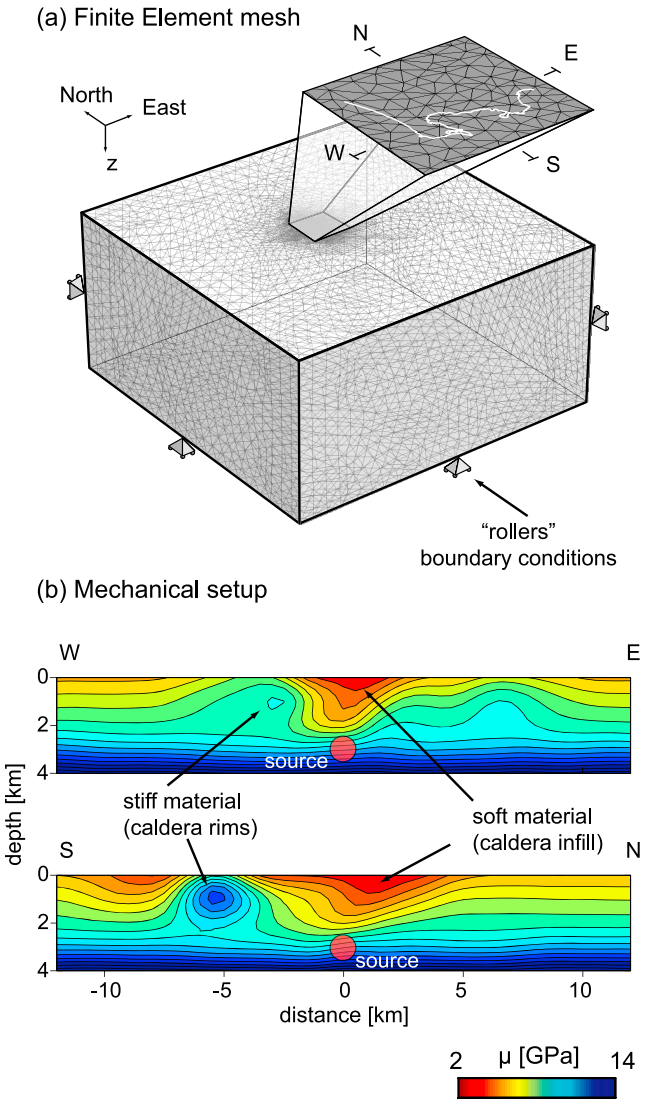

Figure 2. Setup of the 3-D finite element models (3DHET). (a) Mesh and boundary conditions. (b) Mechanical configuration of 3DHET represented here by the distribution of the shear modulus (μ) along two profiles, west-east and south-north, respectively. Poisson's ratios (ν) vary in the range of 0.2–0.4. A positive volume (1 Mm^3) is imposed to a spherical reservoir located in the center of the caldera basin at 3 km depth (see text for more details).

within a small spherical source, located beneath the center of the 3DHET model at 3 km depth, and then solved for the deformation field. Since our analysis will focus on the source assessment by using the SBAS-DInSAR data set for CF caldera (see the following section 3), the synthetic displacements have been projected on the line-of-sight (LOS) of the viewing geometries of available SAR acquisitions, referred to as the ascending and descending satellite's orbits. The synthetic displacements have been thus re-sampled on a uniform grid spaced at 0.5 km, which is a good compromise between the mechanical setup and deformation measurement spatial density, i.e., ~1 km spacing for the seismic tomography and ~0.1 km for the SBAS-DInSAR data. Moreover, we added to the synthetic displacements a random noise, whose standard deviation is on the same order of the accuracies of the SBAS-DInSAR technique (see section 3). We minimized the difference between surface displacements caused by the dilatation of a point source embedded in a homogeneous half-space [*Mogi*, 1958] and the synthetic data by applying an optimization procedure based on a Genetic Algorithm (GA) [*Holland*, 1975], which is a standard and efficient tool in geodetic problems [e.g., *Shirzaei and Walter*, 2009]. We used the L^2 norm as cost function, inferring the confidence interval for the estimated parameters from the range of values of the models that fall within 10% of the minimum cost [*Picozzi et al.*, 2005].

[10] The results of the synthetic tests show very good agreement between the modeled surface deformation, retrieved following the optimization procedure, and the initial synthetic data (Figure 3). Moreover, the estimated values for easting, northing and depth of the source are in agreement with the imposed initial values (Table 1). However, the estimated ΔV results are up to 35% larger than expected. Additional tests, assuming larger signal-to-noise ratio, and/or increasing/decreasing the mechanical contrast between the inner and the outer part of the caldera, achieved similar results. This suggests that the assumption of homogeneous mechanical properties in the analysis of the geodetic data at CF caldera, typically applied when using a "standard" approach, does not affect the assessment of the source location, but might mislead its strength, retrieving values that are likely larger than the "real" ones.

2.2. "Correction" for the 3-D Heterogeneity Effects

[11] Following the results of the synthetic test, in order to retrieve proper estimations also for the values of ΔV,

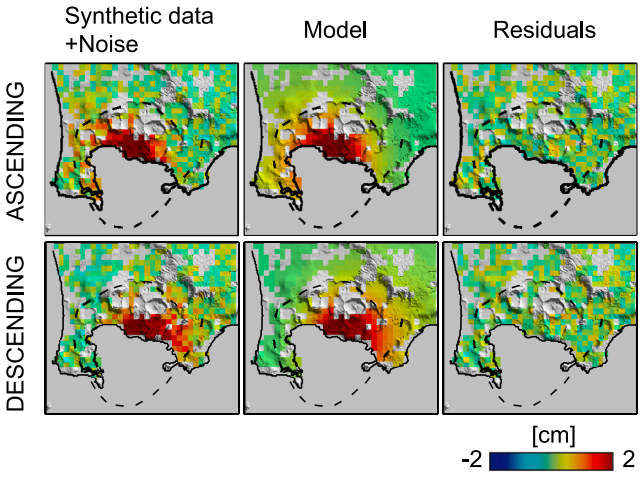

Figure 3. Results of FE synthetic tests. (left) Synthetic data + noise. Synthetic deformation generated on 3DHET model by a volume change on a spherical source, added with random noise and projected on ascending and descending satellites orbit. (middle) Model. Best fit model resulting from the inversion of the synthetic deformation field assuming an isotropic point source embedded on a homogeneous half-space. (right) Residuals. RMS of the differences between synthetic data + noise and model is below 0.3 cm. See also Table 1 and text for more details.

Table 1. Range of Parameters Obtained by the Inversion of the Synthetic Displacements[a]

East (ref 426.82) (km)		North (ref 4519.3) (km)		Depth (ref 3.0) (km)		ΔV (ref 1.0) (Mm^3)		rms
Min	Max	Min	Max	Min	Max	Min	Max	(cm)
426.4	426.9	4519.2	4519.5	2.8	3.1	1.15	1.35	0.3

[a]The initial reference values imposed in the 3DHET model are also reported. While the source position is well constrained from the homogeneous half-space assumption, the volume change is overestimated.

we propose to apply to the data a "correction" function defined as:

$$U_{corrected(E,N)} = U_{InSAR(E,N)} - \frac{K_{(E,N)} \cdot \max\left(U_{InSAR(E,N)}\right)}{w} \quad (1)$$

where U_{InSAR} are the displacements measured at the surface (z = 0), K and w are respectively a "correction" function and a weighting factor that depend on the 3-D mechanical heterogeneity distribution inside the CF caldera, and $U_{corrected}$ are the data "corrected" for the 3-D mechanical heterogeneities effects (details about the determination of K and w are discussed in Appendix A). We repeated the test described in 2.1, applying (1) to the synthetic displacements, and found that all source parameters within the HHS result now in agreement with those considered in the 3DHET forward model. In section 3, the same approach is applied on the real deformation field measured at CF caldera.

3. Analysis of the CF Caldera SBAS-DInSAR Data Set

[12] SBAS-DInSAR approach involves the selection of SAR image pairs to generate interferograms, which are characterized by a small temporal and spatial separation between the acquisition orbits [*Berardino et al.*, 2002]. By exploiting its capability to include images acquired with different SAR sensors [*Pepe et al.*, 2005], we applied SBAS-DInSAR technique to a set of 165 ERS and 62 ENVISAT SAR data acquired between 1992 and 2008 on ascending (track 129, frame 809) and descending (track 36, frame 2781) orbits. The final products are mean ground velocity maps, as well as pixel-wise displacements relative to every acquisition date, which provide a dense spatial and temporal resolution of the surface deformation field. The accuracy of the technique has been quantified to be ± 0.5 cm and ± 0.1 cm/yr for the measured ground displacements and velocities, respectively [*Casu et al.*, 2006].

[13] Figures 4a–4b shows mean ground velocity maps for CF caldera retrieved on the ascending and descending track. Both images evidence an ongoing subsidence with an average velocity up to 2 cm/year, which is the dominating trend of the last 16-years. However, the displacement time series also show a nonlinear behavior (Figures 4c–4d), and provide details about of the evolution of two well-known recent uplift periods in 2000 and 2004–2006 [cf. *Lanari et al.*, 2004; *Trasatti et al.*, 2008].

[14] The SBAS-DInSAR data has been analyzed following the same algorithm explained for the synthetic tests (section 2.1), considering now two distinct procedures: (1) stepwise inversion of the cumulative displacements, where every step corresponds to the date of acquisition, and (2) inversion of mean velocities retrieved on sub-periods with a signal larger than 1 cm/year. For case 1, the full data set resolution has been considered (pixel dimension ca. 0.1x0.1 km), inverting the ascending and descending information separately. For case 2, ascending and descending velocities have been resampled at a lower resolution (0.5x0.5 km) and jointly inverted (same as applied in section 2 for the synthetic tests). The results of both procedures are comparable thus, for clarity, in Figure 5 and Tables 2 and 3 we present only those relevant to the case 2, which are the best representative of the whole performed analysis on the SBAS-DInSAR time series of CF caldera.

[15] In general, the residuals (see Figures 5a–5g) demonstrate the good agreement between models and observations. Northing and easting of the source remain stable during the entire period, moreover, the source depth is constrained between 2.5 and 3.5 km (see Figure 5h). ΔV follows the subsidence and uplift phases, imaging the nonlinearity of the behavior of the source at depth. Note that the application of the "correction" function to the measured data does not affect the estimations of the source location compared to the results obtained with the "standard" approach. On the contrary, the "correction" applied to the data affects the values of ΔV, which are remarkably smaller than those retrieved with the "standard" approach, as hypothesized from the results of the synthetic test (section 2.1). This confirms the applicability of the proposed "correction" method to a data set of real measured data. Moreover, the effect of 3-D mechanical heterogeneities on ΔV estimations involves a number of important implications for the assessment of CF caldera deformation source, which will be discussed in the following sections.

4. Summary and Discussion

[16] In this work, we constructed 3-D finite element models representative of the mechanical setup of the CF caldera (3DHET), by considering a realistic distribution of vertical and lateral mechanical heterogeneities derived from seismic tomography. Standard homogeneous half-space models (HHS), herein used for the interpretation of surface deformation generated within 3DHET, achieved very good assessment of the source location but remarkable overestimation of the source volume change. Thus, we proposed an approach to "correct" the measured data, allowing the use of homogeneous models to retrieve in a fast and reliable way source parameters as they were calculated in a fully 3-D heterogeneous medium. Using this technique, we analyzed the ground displacements measured via SBAS-DInSAR at CF caldera in the period 1992–2008. The dilatation and contraction of a small spherical source, almost stable in position during the entire period of observation, well explains the deformation signal over space and time, achieving small differences between the modeled and the observed data. In the following, we compare our findings to previous studies, discussing the limitations and the validity of our results.

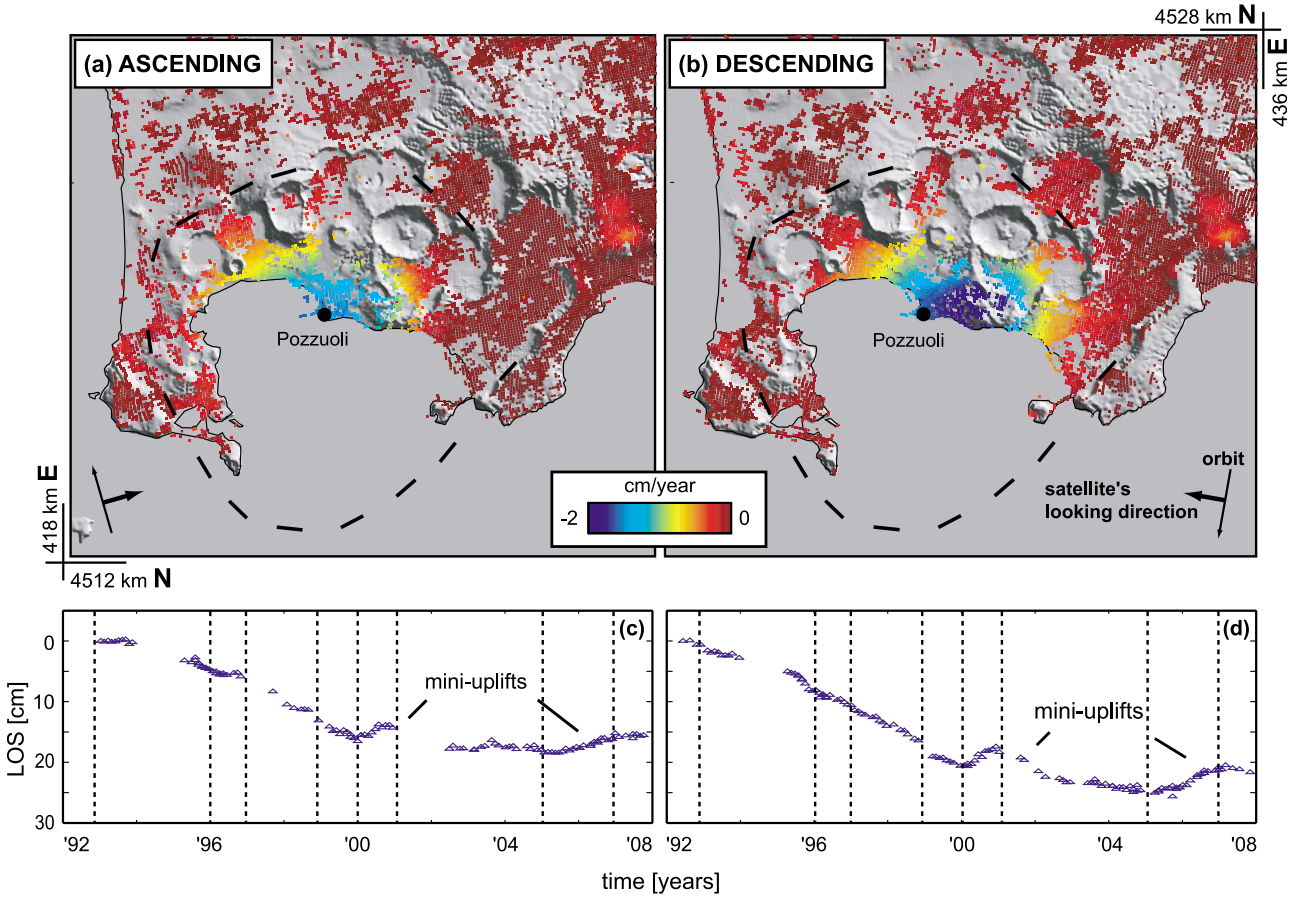

Figure 4. Mean deformation velocity maps superimposed on the digital elevation model of the Campi Flegrei caldera. The deformation field is computed by means of the SBAS-DInSAR technique on (a) ascending and (b) descending images acquired between 1992 and 2008 (see text for more details). (c and d) Time series relevant to the two pixels where the largest velocities are measured for the ascending (Figure 4c) and descending (Figure 4d) orbits. Both time series clearly show a sub-linear subsidence trend (1992–2000) interrupted by two uplift phases in 2000–2001 and 2004–2006.

4.1. Effect Of Mechanical Heterogeneities on Different Source Shapes and Positions

[17] The analyses presented here for the CF caldera example focus on the consideration of a reservoir approximated as a small spherical source. Nevertheless, we also considered in our tests the possibility of larger and/or ellipsoidal shaped sources, keeping them compatible in dimension and position with the a priori information available from the tomography study of *Chiarabba and Moretti* [2006], which is our reference for the CF shallow crustal structure. The results show that assuming synthetic displacements generated by a ΔV of an oblate- and/or prolate-shaped source embedded in a 3DHET model, and inverting for a generic ellipsoidal source embedded in a HHS [*Davis*, 1986; *Yang et al.*, 1988: *Newman et al.*, 2006], the source position, as well as the geometrical parameters (horizontal/vertical semiaxis) are only slightly affected (see also Table 4). Moreover, assuming as initial source larger reservoirs (up to 1 km major semiaxis) and keeping ΔV constant, the differences revealed on surface deformations are smaller than 0.1 mm, which is below accuracies achievable with standard geodetic measurements, thus unlikely affecting source

Figure 5. Results of the inversion after the application of the "correction" function to take into account the 3-D material heterogeneities. (a–g) Data "corrected" ($U_{corrected}$), models and residual maps relative to the inversion of the data stacks, as best representative of the entire analysis of the deformation at Campi Flegrei caldera in the period 1992–2008. See also text for more details. (h) Source parameters: In blue, the parameters of the best fitting models using the "standard" approach (U_{InSAR}). In red, the parameters of the best fitting models after the application of the "correction" function to take into account the 3-D mechanical heterogeneities of the area ($U_{corrected}$). In the background, shaded, result relative to the stepwise inversion of the cumulative displacements, case 1. In the foreground, result relative to the inversion of the data stacks, case 2. See text for details. Error bars represent the range of values that the parameters assumed within the 10% of the minimum cost. Note that easting, northing and source depth are similar in both cases, while the volume changes are smaller when the "correction" for the 3-D material heterogeneities is considered.

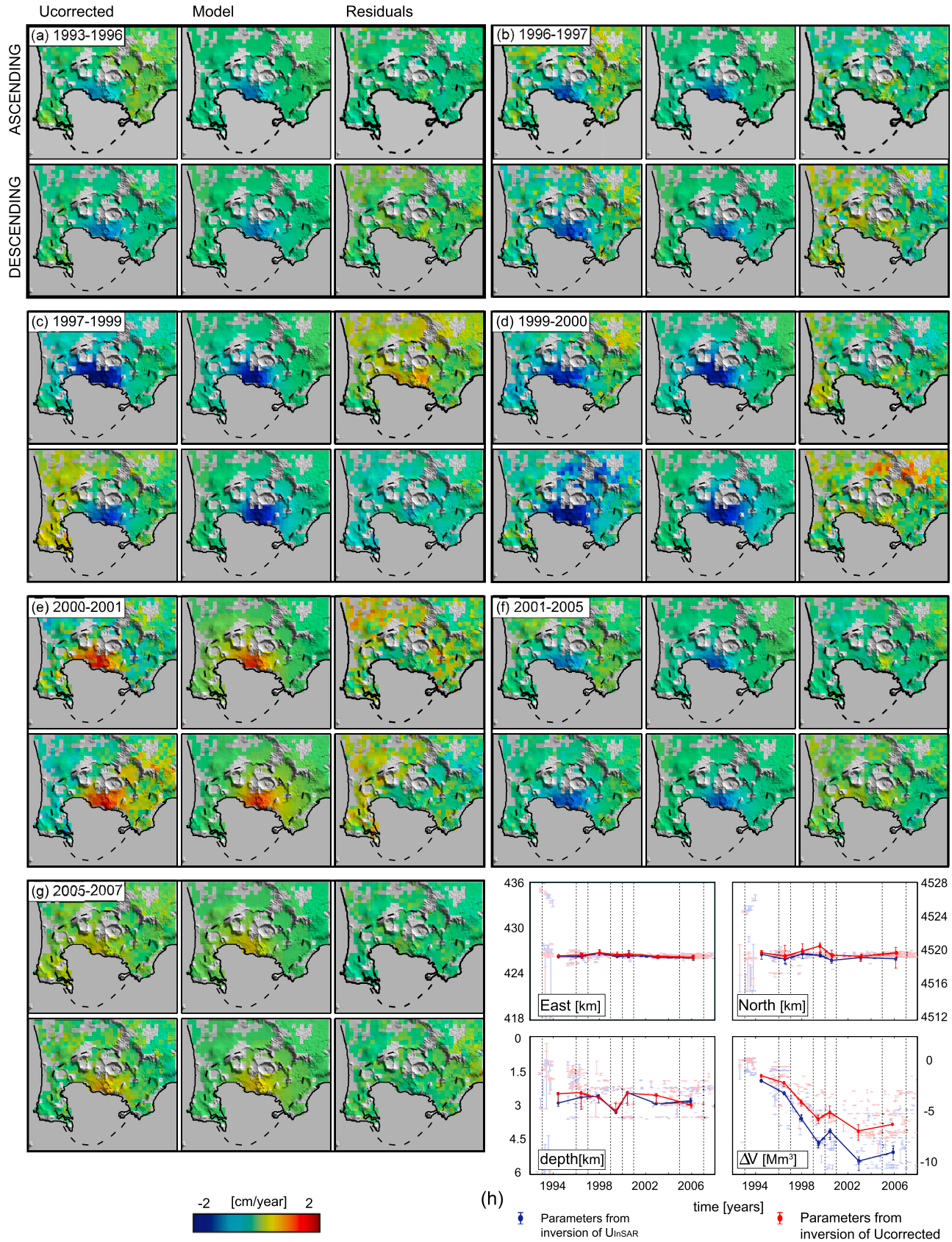
Ucorrected
Model
Residuals
ASCENDING
DESCENDING
(a) 1993-1996
(b) 1996-1997
(c) 1997-1999
(d) 1999-2000
(e) 2000-2001
(f) 2001-2005
(g) 2005-2007
-2 [cm/year] 2
(h)
East [km]
North [km]
depth[km]
ΔV [Mm³]
time [years]
Parameters from inversion of UInSAR
Parameters from inversion of Ucorrected

Figure 5

Table 2. Inversion U_{InSAR}[a]

	East (km)		North (km)		Depth (km)		ΔV (Mm^3/yr)		rms
Period	Min	Max	Min	Max	Min	Max	Min	Max	(cm)
93–96	426.3	426.6	4519.1	4519.6	2.5	3	−0.49	−0.46	0.12
96–97	426.3	426.5	4518.7	4519.4	2.7	3.2	−0.74	−0.65	0.26
97–99	426.6	427.3	4519.2	4520	2.6	3	−1.05	−0.88	0.33
99–00	426.4	426.8	4519.5	4520.2	3.4	3.5	−1.3	−1.25	0.27
00–01	426.3	427.2	4518.9	4519.1	2.5	3	0.53	0.7	0.31
01–05	426.2	426.7	4519	4519.4	2.6	3	−0.7	−0.63	0.16
05–07	425.9	426.5	4519	4519.2	2.8	3	0.31	0.32	0.12

[a]Source parameters obtained by the inversion of the Campi Flegrei deformation assuming the standard approach.

Table 3. Inversion $U_{corrected}$[a]

	East (km)		North (km)		Depth (km)		ΔV (Mm^3/yr)		rms
Period	Min	Max	Min	Max	Min	Max	Min	Max	(cm)
93–96	426.5	426.6	4520	4520.2	2.5	3	−0.35	−0.28	0.12
96–97	426.2	426.9	4519.5	4520.7	2.5	3.1	−0.45	−0.37	0.26
97–99	426.8	427.3	4520.1	4520.8	2.6	2.9	−0.68	−0.59	0.31
99–00	426.6	427	4520	4520.9	2.9	3.4	−0.92	−0.83	0.30
00–01	426.5	427.2	4519	4520.2	2.5	3	0.3	0.48	0.31
01–05	426.2	426.7	4519.2	4519.7	2.6	3	−0.47	−0.39	0.14
05–07	426.1	426.7	4518.6	4520.5	3	3.2	0.21	0.29	0.12

[a]Source parameters obtained by the inversion of the SBAS-DInSAR data "corrected" for the 3-D heterogeneities effects. See also Figure 5.

parameters retrieved by standard optimization procedures. In addition, changing randomly the initial coordinates of the source within the caldera basin in the forward 3DHET model, we found that the position is constrained accurately by the optimization procedure in the 95% of the cases.

[18] In all the above listed tests, the ΔV retrieved from the inversion of synthetic displacements generated within a 3DHET assuming an HHS instead are systematically overestimated, with the largest values while considering an oblate-shaped source (see Table 4). Since the surface deformation is linearly dependent with ΔV, our results suggest that the approach of using "correction" functions as herein proposed (section 2.2.) is thus applicable not only for a small spherical source case, but also for other sources dissimilar in dimensions, shape and position, provided that these characteristics are compatible with the current understanding of the sub-surface crustal structure of CF caldera (see also the following 4.2 section).

[19] Concerning the real measured displacements in the period 1992–2008, previous analysis of portions of the same SBAS-DInSAR data set [*Lundgren et al.*, 2001; *Lanari et al.*, 2004; *Trasatti et al.*, 2008], as well as studies considering different geodetic data sets [*Battaglia et al.*, 2006; *Amoruso et al.*, 2007] found CF caldera source positions very similar to these herein presented, proposing however a range of shapes and dimension that are sometimes in disagreement. This demonstrates that, due the intrinsic non-uniqueness of solutions obtained considering geodetic data only, the estimation of the geometrical parameters associated with more-complex source shapes is very uncertain. For this reason, we present only the best fit results assuming the simplest possible shape, i.e., a small spherical source. We cannot exclude different source geometries or mechanism, such as the intrusion of magmas in the form of extended sill-shaped fractures [*Amoruso et al.*, 2007], or the presence of multiple sources [*Gottsmann et al.*, 2006; *Zollo et al.*, 2008], however we could not distinguish among these scenarios using the available information only. Nevertheless, our results for small spherical source are in agreement with the current understanding of CF unrest phases constrained by independent data (see section 4.3). Further discussion about the modeling assumptions can be found in the Appendix B.

4.2. "Correction" Functions: An Alternative Approach to Account for Material Heterogeneities?

[20] The synthetic tests based on FE evidenced the importance to take into account vertical and lateral mechanical heterogeneities in surface deformation studies at CF caldera. Our interpretation is that the structure of the softer caldera basin, bounded by the stiffer periphery, locally amplifies the surface displacements and leads to major differences while compared with a uniform homogeneous half-space models. Such effects are to some extent analogous to those hypothesized by other authors as the consequence of ring fault dislocation, which, similarly to sharp mechanical contrasts, may cause amplifications and discontinuities on CF caldera stress and strain field [*Beauducel et al.*, 2004]. Thus, we demonstrated that the application of specific "correction" functions to the real measured displacements could be considered as a convenient way to take into account these effects. A straightforward approach would imply the use of 3-D heterogeneous FE models directly within the optimization algorithm; however, the analysis of large data sets, as the 16 year time series for CF caldera here presented, would have been very difficult due to tremendous computational times. The advantage of the proposed technique is that, after the determination of the "correction" functions, the assessment of source parameters can be still performed by using simplified models. This is particularly convenient for monitoring purposes, where a fast and reliable quantitative analysis is needed. Such approach is to some extent similar to seismology applications, where "correction" functions are used to compensate for the effects

Table 4. Synthetic Test With Different Source Shape[a]

	Hor/Vert Semiaxis	ΔV
3DHET	1	
HHS	0.85–1.1	+25–37%
3DHET	2	
HHS	1.9–2.3	+50–200%
3DHET	0.5	
HHS	0.3–0.8	+10–25%

[a]Results of the synthetic tests assuming spheroidal sources with different semiaxis ratios within the 3-D heterogeneous models (3DHET) and inverting for a generic ellipsoidal source embedded in a homogeneous half-space (HHS). Source position and geometrical parameters (here summarized by the horizontal/vertical semiaxis ratio) are well constrained within the HHS, suggesting that mechanical heterogeneities only slightly affect these parameters. However, the ΔV is systematically overestimated by the assumption of mechanical homogeneity. The conversion from ΔP to ΔV is calculated by considering the relationships proposed by *Amoruso and Crescentini* [2009].

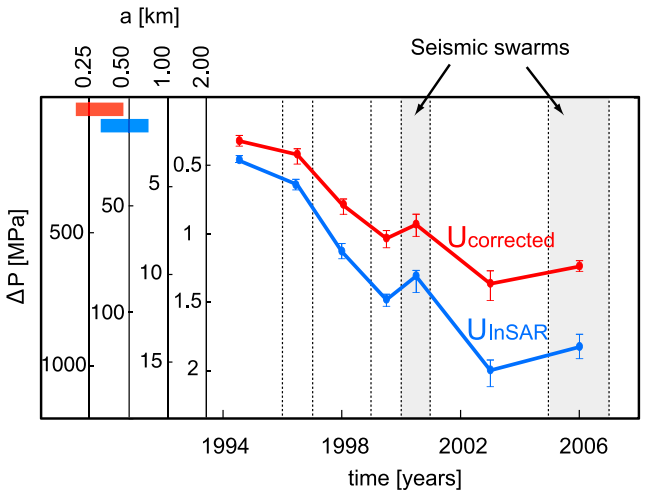

Figure 6. Pressures changes (ΔP) of a spherical source located at about 3 km depth beneath CF caldera between 1992 and 2008. ΔP has been calculated with relation (A2) (see Appendix A) considering the ΔV resulting from the inversion of the SBAS-DInSAR data set for the "standard" approach (blue solid line) and after the "correction" procedure (red solid line) for a shear modulus (μ) of 7 GPa. Since ΔP depends also from the source radius, the range $0.25 < a < 2$ km has been evaluated; thus the vertical axis is scaled accordingly. Among the source radii considered, the values consistent with ΔP range of 10–30 MPa, thus explaining the seismicity observed at Campi Flegrei during the 2000–2001 uplift phase [*Bianco et al.*, 2004], are shown by the blue and red bars in the top left corner. See also text for more details.

of lateral variations in the crust and uppermost mantle on wave travel times [*Wright*, 2008 and references therein].

[21] The method herein presented can be applied to other volcanic areas where mechanical heterogeneities have no effect on the estimation of the source location and geometry. In general, we argue that for other calderas, where often an inner basin with softer mechanical properties bounded by stiffer materials on the caldera rims is present (e.g., Yellowstone or Long Valley), an analogous behavior as shown here for CF might be expected. In addition, the method can be applied to any other geodetic signal (e.g., leveling, GPS), and also to any other model that assumes linear relationship between surface deformation and source strength (see also section 4.1). However, since mechanical heterogeneities might mislead also the source's depth [*Manconi et al.*, 2007; *Masterlark*, 2007], a quantitative evaluation requires always a priori geophysical investigations and numerical tests, in order to characterize the "realistic" mechanical behavior in turn for each volcanic area.

4.3. Constraints on the Evolution of Pressures at Depth in the Last 16 Years

[22] Using the results of the inversion of the SBAS-DInSAR time series "corrected" for the 3-D heterogeneities effects, we can derive additional information about the source responsible for the deformation observed at CF caldera in the past 16 years. Figure 6 shows the evolution of the pressure changes (ΔP) at CF caldera occurring at depths of about 3 km in the period between 1992 and 2008, which have been obtained from the relationship between and ΔV and ΔP for a spherical source (see equation (A2)). As shear modulus (μ), we herein considered $\mu = 7$ GPa, an average of the values derived from the seismic tomography in the near field, i.e., ± 8 km from the center of the caldera up to 4 km depth, weighted by the resolution of the grid used for the seismic tomography itself (1x1x1 km). This is in agreement with realistic values of μ proposed for CF caldera, which span between 1 GPa and 15 GPa [*Amoruso et al.*, 2008; *Trasatti and Bonafede*, 2008]. However, since the mechanical properties, as well as the source shape considered, might largely affect the ΔP estimate, the analysis described in this section has to be considered as qualitative (see also Appendix B). In this context, we may select an appropriate value of source radius considering the a priori information available from independent geophysical studies in the area. For example, the seismicity recorded during the uplift phase of 2000–2001 indicates values of ΔP in the order of 10–30 MPa at 3 km depth [*Saccorotti et al.*, 2001; *Bianco et al.*, 2004]. The earthquakes have been related to an increase of hydrostatic fluid pressure (ΔP) within the CF caldera hydrothermal system, thought to be energetic enough to induce fluid migration and brittle failure of the rocks hosting the fluid-filled cavities [*Bianco et al.*, 2004]. If we assume that the sources of the deformation and of the seismicity are the same, i.e., a pressure change within a reservoir, considering a range of radii between 0.25 and 2 km and calculating the relative ΔP with the relationship given in (A2), we can compare the values obtained from our study to these proposed by *Bianco et al.* [2004]. To achieve the ΔP range of 10–30 MPa, for the "standard" approach (blue bar, Figure 6, top left corner) the source radius results smaller than 1 km. The consideration of 3-D heterogeneities constrains the source radius to values as smaller as 0.5 km (red bar, Figure 6, top left corner). Such source dimension is rather compatible with the seismic velocity anomaly located in the center of the caldera at about 2.5–3.5 km depth, evidenced from seismic tomography and recent seismic reflection studies [*Chiarabba and Moretti*, 2006; *Zollo et al.*, 2008]. In other words, the pressurized reservoir is very small and unlikely related to a major magma plumbing system, in agreement also with other independent data. Indeed, this anomaly has been interpreted as a rock volume filled with over-pressurized gas and fluids, probably related to the hydrothermal reservoir of the CF caldera system, hypothesized to react in response to the activity of a deeper magmatic body [e.g., *De Natale et al.*, 2006, and references therein]. Such interpretation is further supported by recently published geochemical data retrieved from the monitoring of the active fumarolic field over the same time period [*Chiodini*, 2009].

5. Conclusions

[23] The main conclusions of this work can be summarized as follows:

[24] 1. In the study of surface deformations at CF caldera, the assumption of a homogeneous half-space does not affect the estimation of the source location, but mislead the assessment of source's strength.

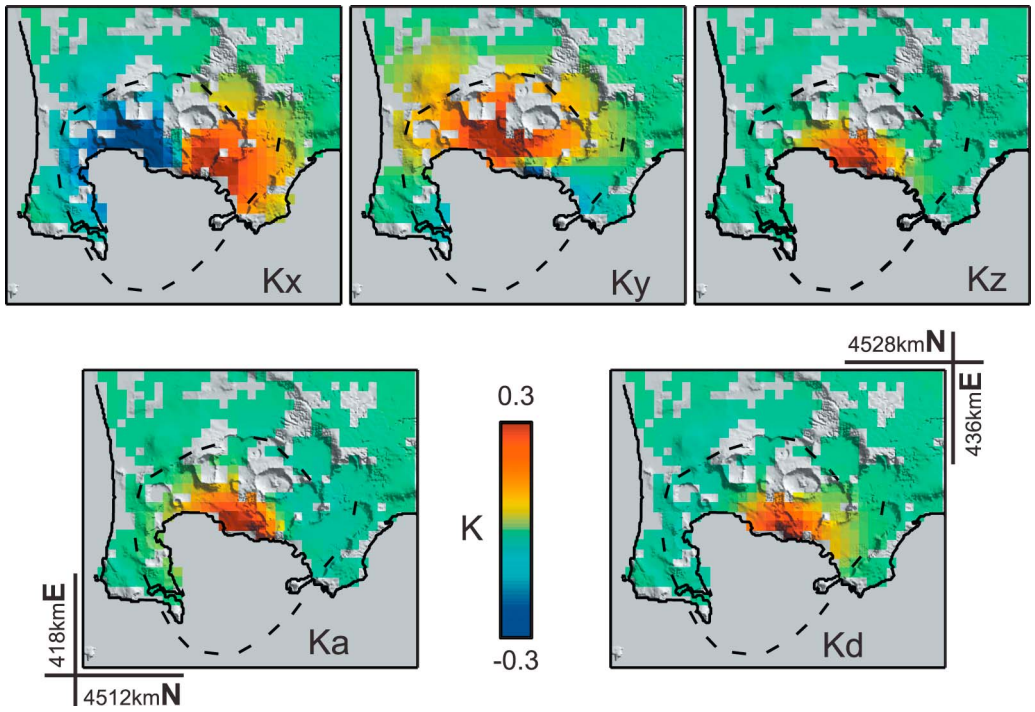

Figure A1. Correction functions (see equation (A4)) superimposed on the digital elevation model of the Campi Flegrei caldera for the three components of the displacement field (Kx, Ky, and Kz) and projected on the ascending (Ka) and descending (Kd) satellite viewing geometries.

[25] 2. The surface deformation measured by means of geodetic techniques at CF caldera can be "corrected" with specific functions to take into account the effects of 3-D heterogeneities, thus obtaining fast and reliable estimations also for the source strength.

[26] 3. The analysis of the complete CF caldera SBAS-DInSAR data set suggests that all the deformation observed between 1992 and 2008 is probably entirely related to the unrests of a small source located in the center of the caldera at about 3 km depth. The pressure variations estimated in this study are compatible with those believed to cause the seismic swarms during the uplift periods, which are likely related to hydrostatic pressure variations occurred within the hydrothermal reservoir.

Appendix A: Details on the Estimations of the "Correction" Function

[27] The "correction" function used for the displacements measured at CF caldera has been derived after several empirical tests performed using FE models. In this appendix, we explain the procedure adopted for such purpose. Starting from the analytical model of a small spherical cavity embedded in an elastic homogeneous medium [*Mogi*, 1958], we can write

$$U_{(E,N)} = G \cdot s \tag{A1}$$

where $U_{(E,N)}$ are the surface displacements, G are the Green's functions for displacements, which depend on the source position with respect to the free surface and on the half-space elastic properties, and s is the strength of the dilatation/contraction source. The latter might be described in terms of volume or pressure changes:

$$s = \Delta P(1-\upsilon)\frac{a^3}{\mu} = \Delta V \frac{(1-\upsilon)(1+\upsilon)}{2\pi(1-2\upsilon)} \tag{A2}$$

where ΔP and ΔV are the pressure and the volume change, respectively, a is the radius of the source, μ is the shear modulus and ν is the Poisson's ratio which both depend on the elastic characteristics of the half-space [cf. *Masterlark*, 2007].

[28] Setting up two FE models and considering for both the same source parameters, i.e., location and strength s, but different mechanical setups, using the same notation as for equation (A1) we may write

$$\begin{aligned} U_{3DHET(E,N)} &= G^*_{3DHET} \cdot s \\ U_{HHS(E,N)} &= G^*_{HHS} \cdot s \end{aligned} \tag{A3}$$

where 3DHET and HHS stay respectively for the 3-D heterogeneous and for the average homogeneous half-space mechanical configurations, and G* stays for the reduced Green's functions, which now depend only on the elastic constants. Due to the linear relationship between the surface displacements and the source strength, when linear elastic material is assumed, the relationship

$$K_{(E,N)} = \frac{U_{3DHET(E,N)}}{\max\left(U_{HHS(E,N)}\right)} - \frac{U_{HHS(E,N)}}{\max\left(U_{HHS(E,N)}\right)} \tag{A4}$$

is a representative of the normalized difference between the two assumed mechanical setups, while

$$w = \frac{\max\left(U_{3DHET(E,N)}\right)}{\max\left(U_{HHS(E,N)}\right)} \quad \text{(A5)}$$

is a weighting factor representative of amplification (positive) or decrease (negative) of the surface displacements. In a real case, we measure the surface deformations with a geodetic technique, e.g., DInSAR (U_{InSAR}). Assuming that the 3DHET model achieves a realistic representation of the deformations occurring in reality, we may substitute U_{3DHET} with U_{InSAR}, and thus derive

$$U_{corrected(E,N)} = U_{InSAR(E,N)} - \frac{K_{(E,N)} \cdot \max\left(U_{InSAR(E,N)}\right)}{w} \quad \text{(A6)}$$

The values of K, calculated for the three deformation components (Kx, Ky, and Kz) and on ascending (Ka) and descending (Kd) satellite's LOS directions, are shown in Figure A1. The factor w assumes the value 1.32 for the ascending and 1.34 for the descending viewing geometries. K and w depend on the average value of the shear modulus μ selected as HHS representative for the 3-D heterogeneous distribution. In summary, if the material properties are not affecting the estimation the source location, and if the position of the source is not changing during the period of observation, as demonstrated from the analysis of the SBAS-DInSAR data set of CF caldera, the inversion of $U_{corrected}$ retrieves values of ΔV corrected for the effects of 3-D mechanical heterogeneities.

Appendix B: Finite Element Modeling Assumptions and Mechanical Setup

[30] Recent studies analyzed the influence of 1-D layering (only vertical heterogeneities) on the estimation of source parameters at CF caldera [*Crescentini and Amoruso*, 2007]. We compared our 3DHET model with an approximated 1-D layered configuration, finding that the latter attains displacements up to 15% smaller in the inner caldera. Hence, a more realistic mechanical setup detailed from the 3-D tomography study, as considered in our FE models, provides better constraints on the strain behavior of the CF caldera. However, the material properties derived from seismic tomography might be biased by the resolution of the tomographic study itself. Nevertheless, we consider the velocity model of *Chiarabba and Moretti* [2006] to date one of the best available representations of the 3-D structure of CF caldera. An improvement of the resolution of tomographic analysis may allow constructing FE models with a more detailed mechanical setup, thus a better assessment of 3-D heterogeneities effects. In any case, the elastic constants derived from seismic velocities are representative for the undrained response of rocks to a dynamic stress solicitation. Deformation caused by volcanic sources, in turn, assumes a relatively constant application of stress over a longer time. Therefore, the consideration of static and drained response would be more appropriate in the analysis of the displacement field [*Heap et al.*, 2009]. Specific laboratory tests constraining static elastic properties for CF caldera are unfortunately at the moment not available. Static versus dynamic mechanical parameters might be in some cases similar, but they might also differ by up to 1–2 order of magnitude, especially where the materials are subjected to plastic rather than pure elastic deformation [*McCann and Entwisle*, 1992; *Soroush and Fahimifar*, 2003]. Thus, the elastic mechanical parameters herein used, in agreement with those derived using ultrasonic logs in laboratory experiments, might be considered as an upper limit for the material properties of CF caldera [*Zamora et al.*, 1994].

[31] The assumption of drained response of rocks to stress solicitations would imply the assumption of Poisson's ratio $\nu = 0.25$ throughout the models [e.g., *Trasatti et al.*, 2005]. However, recent laboratory experiments on volcanic rock samples have shown that cyclic loading may increase ν by up a factor of 3, independently on drained or undrained conditions [*Heap et al.*, 2009]. For this reason, it is difficult to distinguish what might be the causes of the relatively large values of ν resulting from the conversion of the seismic velocities, as in the upper levels of CF caldera. In fact, they might be related not only to the presence of fluids, hence undrained response, but also due to the effects of cyclic loading caused by the recurrent uplift and subsidence phases experienced by this area. We note, however, that the consideration of $\nu = 0.25$ in the whole domain of 3DHET had no remarkable effects on our final results.

[32] Time-and-temperature dependent material properties, as poroelastic, viscoelastic and viscoplastic behavior might also have major effects on CF caldera strain behavior, hence on the evaluation of source processes [*Bonafede*, 1991; *De Natale et al.*, 1991]. The parameters to accomplish more detailed analyses are still poorly constrained. Further investigations are needed to better assess the effects of such complexities on behavior of the source and of the deformation field at CF caldera.

[33] **Acknowledgments.** The SAR images for the SBAS-DInSAR analysis were provided by the ESA as part of CAT-1 project 4532. Thanks to K. Burjorjee for the implementation of the GA in the Matlab programming language (vector-GA, open-source project available at http://code.google.com/p/vector-ga/). The finite element models presented here to investigate CF caldera's ground deformation have been implemented by using the Structural Mechanics module of the Comsol Multiphysics™ package (available at http://www.comsol.com). Thanks to C. Chiarabba and M. Moretti for the seismic tomography data. We acknowledge fruitful discussions with A. Amoruso, L. Crescentini, T. Masterlark, M. Heap, J. Ruch, M. Picozzi, S. Parolai, M. Shirzaei, and R. Wang. German Research Foundation (DFG grant WA1642-1/4), ASI-SRV, the Italian DPC, and the GFZ German Centre for Geosciences have financially supported this work.

References

Amoruso, A., and L. Crescentini (2009), Shape and volume change of pressurized ellipsoidal cavities from deformation and seismic data, *J. Geophys. Res.*, *114*, B02210, doi:10.1029/2008JB005946.

Amoruso, A., L. Crescentini, A. T. Linde, I. S. Sacks, R. Scarpa, and P. Romano (2007), A horizontal crack in a layered structure satisfies deformation for the 2004–2006 uplift of Campi Flegrei, *Geophys. Res. Lett.*, *34*, L22313, doi:10.1029/2007GL031644.

Amoruso, A., L. Crescentini, and G. Berrino (2008), Simultaneous inversion of deformation and gravity changes in a horizontally layered halfspace: Evidences for magma intrusion during the 1982–1984 unrest at Campi Flegrei caldera (Italy), *Earth Planet. Sci. Lett.*, *272*(1–2), 181–188, doi:10.1016/j.epsl.2008.04.040.

Battaglia, M., C. Troise, F. Obrizzo, F. Pingue, and G. De Natale (2006), Evidence for fluid migration as the source of deformation at Campi Flegrei Caldera, *Geophys. Res. Lett.*, *33*, L01307, doi:10.1029/2005GL024904.

Beauducel, F., G. D. Natale, F. Obrizzo, and F. Pingue (2004), 3-D modelling of Campi Flegrei ground deformations: Role of caldera boundary discontinuities, *Pure Appl. Geophys.*, *161*(7), 1329–1344, doi:10.1007/s00024-004-2507-4.

Bellucci, F., J. Woo, C. R. J. Kilburn, and G. Rolandi (2006), Ground deformation at Campi Flegrei, Italy: Implications for hazard assessment, *Geol. Soc. Spec. Publ.*, *269*(1), 141–157, doi:10.1144/GSL.SP.2006.269.01.09.

Berardino, P., G. Fornaro, R. Lanari, and E. Sansosti (2002), A new algorithm for surface deformation monitoring based on small baseline differential SAR interferograms,, *IEEE Trans. Geosci. Remote Sens.*, *40*(11), 2375–2383, doi:10.1109/TGRS.2002.803792.

Bianco, F., E. Del Pezzo, G. Saccorotti, and G. Ventura (2004), The role of hydrothermal fluids in triggering the July August 2000 seismic swarm at Campi Flegrei, Italy: Evidence from seismological and mesostructural data, *J. Volcanol. Geotherm. Res.*, *133*(1–4), 229–246, doi:10.1016/S0377-0273(03)00400-1.

Bodnar, R. J., C. Cannatelli, B. De Vivo, A. Lima, H. E. Belkin, and A. Milia (2007), Quantitative model for magma degassing and ground deformation (bradyseism) at Campi Flegrei, Italy: Implications for future eruptions, *Geology*, *35*(9), 791–794, doi:10.1130/G23653A.1.

Bonafede, M. (1991), Hot fluid migration: An efficient source of ground deformation: Application to the 1982–1985 crisis at Campi Flegrei-Italy, *J. Volcanol. Geotherm. Res.*, *48*(1–2), 187–198, doi:10.1016/0377-0273(91)90042-X.

Brocher, T. M. (2005), Empirical relations between elastic wavespeeds and density in the Earth's crust, *Bull. Seismol. Soc. Am.*, *95*(6), 2081–2092, doi:10.1785/0120050077.

Casu, F., M. Manzo, and R. Lanari (2006), A quantitative assessment of the SBAS algorithm performance for surface deformation retrieval from DInSAR data, *Remote Sens. Environ.*, *102*(3–4), 195–210, doi:10.1016/j.rse.2006.01.023.

Cayol, V., and F. H. Cornet (1998), Effects of topography on the interpretation of the deformation field of prominent volcanoes: Application to Etna, *Geophys. Res. Lett.*, *25*(11), 1979–1982, doi:10.1029/98GL51512.

Chiarabba, C., and M. Moretti (2006), An insight into the unrest phenomena at the Campi Flegrei caldera from Vp and Vp/Vs tomography, *Terra Nova*, *18*(6), 373–379, doi:10.1111/j.1365-3121.2006.00701.x.

Chiodini, G. (2009), CO_2/CH_4 ratio in fumaroles a powerful tool to detect magma degassing episodes at quiescent volcanoes, *Geophys. Res. Lett.*, *36*, L02302, doi:10.1029/2008GL036347.

Crescentini, L., and A. Amoruso (2007), Effects of crustal layering on the inversion of deformation and gravity data in volcanic areas: An application to the Campi Flegrei caldera, Italy, *Geophys. Res. Lett.*, *34*, L09303, doi:10.1029/2007GL029919.

Davis, P. M. (1986), Surface deformation due to inflation of an arbitrarily oriented triaxial ellipsoidal cavity in an elastic half-space, with reference to Kilauea Volcano, Hawaii, *J. Geophys. Res.*, *91*, 7429–7438, doi:10.1029/JB091iB07p07429.

De Natale, G., F. Pingue, P. Allard, and A. Zollo (1991), Geophysical and geochemical modelling of the 1982–1984 unrest phenomena at Campi Flegrei caldera (southern Italy), *J. Volcanol. Geotherm. Res.*, *48*(1–2), 199–222, doi:10.1016/0377-0273(91)90043-Y.

De Natale, G., C. Troise, F. Pingue, G. Mastrolorenzo, L. Pappalardo, M. Battaglia, and E. Boschi (2006), The Campi Flegrei caldera: Unrest mechanisms and hazards, *Geol. Soc. Spec. Publ.*, *269*(1), 25–45, doi:10.1144/GSL.SP.2006.269.01.03.

Dzurisin, D. (2006), *Volcano Deformation: Geodetic Monitoring Techniques*, 441 pp., Springer, Berlin.

Fagan, M. J. (1992), *Finite Element Analysis: Theory and Practice*, 315 pp., Longman, Harlow, U. K.

Gottsmann, J., A. G. Camacho, K. F. Tiampo, and J. Fernandez (2006), Spatiotemporal variations in vertical gravity gradients at the Campi Flegrei caldera (Italy): A case for source multiplicity during unrest?, *Geophys. J. Int.*, *167*(3), 1089–1096, doi:10.1111/j.1365-246X.2006.03157.x.

Heap, M. J., S. Vinciguerra, and P. Meredith (2009), The evolution of elastic moduli with increasing crack damage during cyclic stressing of a basalt from Mt. Etna volcano, *Tectonophysics*, *471*, 153–160, doi:10.1016/j.tecto.2008.10.004.

Holland, J. H. (1975), *Adaptation in Natural and Artificial Systems*, Univ. of Mich. Press, Ann Arbor.

Lanari, R., P. Berardino, S. Borgström, C. Del Gaudio, P. De Martino, G. Fornaro, S. Guarino, G. P. Ricciardi, E. Sansosti, and P. Lundgren (2004), The use of IFSAR and classical geodetic techniques for caldera unrest episodes: Application to the Campi Flegrei uplift event of 2000, *J. Volcanol. Geotherm. Res.*, *133*(1–4), 247–260, doi:10.1016/S0377-0273(03)00401-3.

Lundgren, P., S. Usai, E. Sansosti, R. Lanari, M. Tesauro, G. Fornaro, and P. Berardino (2001), Modeling surface deformation observed with synthetic aperture radar interferometry at Campi Flegrei caldera, *J. Geophys. Res.*, *106*(B9), 19,355–19,366, doi:10.1029/2001JB000194.

Manconi, A., T. R. Walter, and F. Amelung (2007), Effects of mechanical layering on volcano deformation, *Geophys. J. Int.*, *170*(2), 952–958, doi:10.1111/j.1365-246X.2007.03449.x.

Masterlark, T. (2007), Magma intrusion and deformation predictions: Sensitivities to the Mogi assumptions, *J. Geophys. Res.*, *112*, B06419, doi:10.1029/2006JB004860.

Mastrolorenzo, G., and L. Pappalardo (2006), Magma degassing and crystallization processes during eruptions of high-risk Neapolitan-volcanoes: Evidence of common equilibrium rising processes in alkaline magmas, *Earth Planet. Sci. Lett.*, *250*(1–2), 164–181, doi:10.1016/j.epsl.2006.07.040.

McCann, D. M., and D. C. Entwisle (1992), Determination of Young's modulus of the rock mass from geophysical well logs, *Geol. Soc. Spec. Publ.*, *65*(1), 317–325, doi:10.1144/GSL.SP.1992.065.01.24.

Mogi, K. (1958), Relations between the eruptions of various volcanoes and the deformations of the ground surface around them, *Bull. Earthquake Res. Inst. Univ. Tokyo*, *36*, 99–134.

Newman, A. V., T. H. Dixon, and N. Gourmelen (2006), A four-dimensional viscoelastic deformation model for Long Valley Caldera, California, between 1995 and 2000, *J. Volcanol. Geotherm. Res.*, *150*, 244–269, doi:10.1016/j.jvolgeores.2005.07.017.

Pepe, A., E. Sansosti, P. Berardino, and R. Lanari (2005), On the generation of ERS/ENVISAT DInSAR time-series via the SBAS technique, *Geosci. Remote Sens. Lett.*, *2*(3), 265–269, doi:10.1109/LGRS.2005.848497.

Picozzi, M., S. Parolai, and S. M. Richwalski (2005), Joint inversion of H/V ratios and dispersion curves from seismic noise: Estimating the S-wave velocity of bedrock, *Geophys. Res. Lett.*, *32*, L11308, doi:10.1029/2005GL022878.

Saccorotti, G., F. Bianco, M. Castellano, and E. D. Pezzo (2001), The July August 2000 seismic swarms at Campi Flegrei volcanic complex, Italy, *Geophys. Res. Lett.*, *28*(13), 2525–2528, doi:10.1029/2001GL013053.

Shirzaei, M., and T. R. Walter (2009), Randomly iterated search and statistical competency as powerful inversion tools for deformation source modeling: Application to volcano interferometric synthetic aperture radar data, *J. Geophys. Res.*, *114*, B10401, doi:10.1029/2008JB006071.

Soroush, H., and A. Fahimifar (2003), Evaluation of some physical and mechanical properties of rocks using ultrasonic pulse technique and presenting equations between dynamic and static constants, in *ISRM 2003—Technology Roadmap for Rock Mechanics*, *SAIMM Symp. Ser.*, vol. S33, 6 pp., South Afr. Inst. of Min. and Metall., Johannesburg.

Trasatti, E., and M. Bonafede (2008), Gravity changes due to overpressure sources in 3D heterogeneous media: Application to Campi Flegrei caldera, (Italy), *Ann. Geophys.*, *51*, 121–136.

Trasatti, E., C. Giunchi, and M. Bonafede (2005), Structural and rheological constraints on source depth and overpressure estimates at the Campi Flegrei caldera, Italy, *J. Volcanol. Geotherm. Res.*, *144*(1–4), 105–118, doi:10.1016/j.jvolgeores.2004.11.019.

Trasatti, E., et al. (2008), The 2004–2006 uplift episode at Campi Flegrei caldera (Italy): Constraints from SBAS-DInSAR ENVISAT data and Bayesian source inference, *Geophys. Res. Lett.*, *35*, L07308, doi:10.1029/2007GL033091.

Wright, C. (2008), Station corrections for the Kaapvaal seismic network: Statistical properties and relation to lithospheric structure, *Phys. Earth Planet. Inter.*, *167*(1–2), 39–52, doi:10.1016/j.pepi.2008.02.003.

Yang, X., P. M. Davis, and J. H. Dieterich (1988), Deformation from inflation of a dipping finite prolate spheroid in an elastic half-space as a model for volcanic stressing, *J. Geophys. Res.*, *93*(B5), 4249–4257, doi:10.1029/JB093iB05p04249.

Zamora, M., G. Sartoris, and W. Chelini (1994), Laboratory measurements of ultrasonic wave velocities in rocks from the Campi Flegrei volcanic system and their relation to other field data, *J. Geophys. Res.*, *99*(B7), 13,553–13,561, doi:10.1029/94JB00121.

Zollo, A., N. Maercklin, M. Vassallo, D. D. Iacono, J. Virieux, and P. Gasparini (2008), Seismic reflections reveal a massive melt layer feeding Campi Flegrei caldera, *Geophys. Res. Lett.*, *35*, L12306, doi:10.1029/2008GL034242.

R. Lanari, A. Manconi, M. Manzo, E. Sansosti, P. Tizzani, and G. Zeni, IREA-CNR, Via Diocleziano 328, I-80124 Napoli, Italy. (manconi.a@irea.cnr.it)

T. R. Walter, Department of Physics of the Earth, GFZ German Research Centre for Geoscience, D-14473 Potsdam, Germany.